J. Sci. I. R. Iran

Vol.9 No.4
Autumn 1998

PHYSICO-CHEMICAL CHARACTERISTICS OF MINERALIZING FLUIDS AT THE KAMAR-MEHDI MINE, TABAS REGION, IRAN

F. Moore[1], M. Sadeghi[2] and M. Jami[1]

[1]*Department of Geology, College of Sciences, Shiraz University, Shiraz, Islamic Republic of Iran*
[2]*Department of Mining, College of Engineering & Technology, Birjand University, Birjand, Islamic Republic of Iran*

Abstract

The data obtained from field and geothermometric studies and also the REE composition of fluorites associated with lead mineralization at the Kamar-Mehdi mine are compatible with a structurally controlled, fissure filling, epigenetic, hydrothermal origin. Homogenization and last ice melting temperatures for primary fluid inclusions trapped in fluorite crystals indicate that the mineralization of fluorite and the associated (cogenetic ?) lead has taken place over a temperature range of 115-125°C. The mineralizing fluids were dilute and do not show any apparent change in temperature and salinity with depth. Salinities of inclusion fluids range from 0.7 to 3.7 equivalent wt.% NaCl, and Na/Ca atomic ratio of inclusion leachates is low with all leachates containing appreciable amounts of K and Mg. The daughter minerals are mostly Ca, K, Al, Si, Cl phases.

Introduction

Kamar-Mehdi fluorite mine, the largest of its kind in the area, is located about 100 km southeast of Tabas, in the so-called Tabas Block in central Lut region (56°E, 33°N). This region is an elongate and stable north-south trending block measuring 900 kms along its long axis [14]. Berberian [1] suggests that the Lut region is one of the many results of the Kimmerian orogeny which affected all parts of Iran, except the Zagros Mountain Ranges, in the Middle Triassic epoch. According to Darvishzadeh [4], a stratigraphic characteristic of this region is the presence of Mesozoic sedimentary sequences of considerable thickness. To its west, the thickness of Mesozoic sedimentary layers is in excess of 5000 meters. Tehrani [17] believes that in the Upper Triassic-Lower Jurassic epoch, Shotori Mountain Ranges, acting as a horst structure, divided the Lut region into an eastern Lut Block and a western Tabas Block in which the Kamar-Mehdi anticline occurs.

The spotted schists, phyllites and quartzite of the Tashk Formation, and the slaty shale and quartzite of the Kalmard Formation, both Precambrian in age, represent the oldest exposed Formations in the Tabas Block. However, the oldest formation in the Kamar-Mehdi anticline is Triassic and is divided into two sections, a Middle Triassic (Shotori Formation) and an Upper Triassic (Nayband Formation). Other formations, in descending order of age, comprise Shemshak, Badamo, and Baghamshah Formations (Fig. 1).

Keywords: Fluid inclusion; Fluorite; Kamar Mehdi anticline; Rare Earth Elements

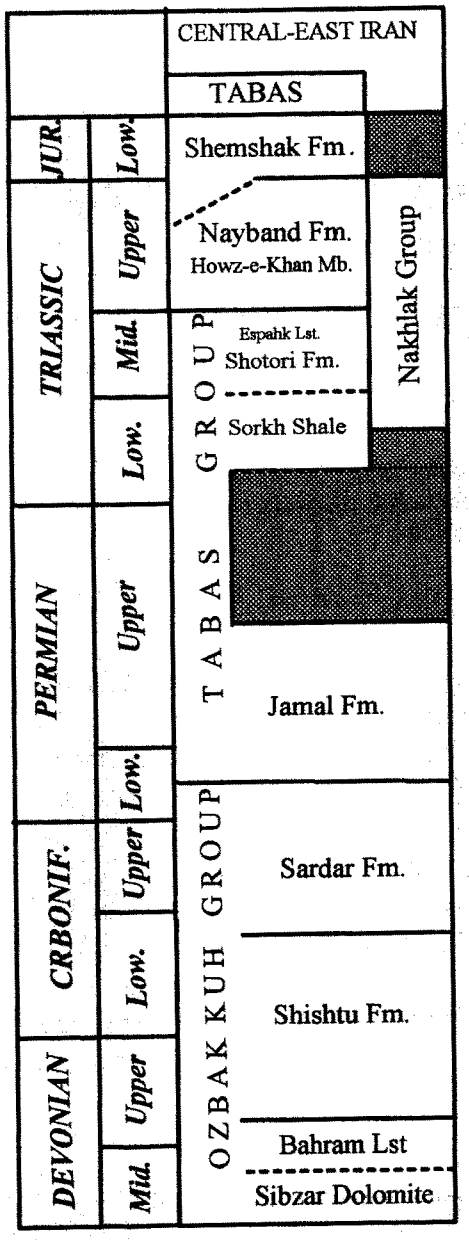

Figure 1. Stratigraphic column of the region (compiled from Stocklin, J. *et al.* 1977)

Kamar-Mehdi anticline is a north-south trending eroded fold exposed at the southwestern end of the Tabas Block. The dolomites of Shotori Formation, which make the core of this doubly-plunging compressional fold and host the fluorite mineralization, are now surrounded by recent alluvium. The eastern and western flanks, made of younger dolomitic rocks, are also covered with alluvium. A thick sequence of Jurassic evaporites consisting mainly of gypsum and gypsyferous marl represent the youngest rocks in the vicinity of the Kamar-Mehdi anticline. This sequence unconformably overlies the older formations [13,15]. Figure 2 depicts the main geological features of the Kamar-Mehdi anticline.

The seemingly structurally controlled mineralization is confined to the east-west trending fault planes that occur in the uniform, well-bedded, dense, yellow dolomite of Shotori Formation, in the core of the anticline. So far, more than 80 east-west trending veins of varying thickness have been identified. The thickness of 14 veins is more than one meter. Fluorite is the main ore mineral, with subordinate galena, magnetite, hematite, pyrite, cerussite, anglesite, malachite, and azurite. The paragenetic sequence of mineralization is presented in Figure 3.

The so-called Kamar-Mehdi mine actually consists of two northern and southern swarms of veins, 10 km apart, and locally known as mine No. 1 and 2, respectively. The southern veins are estimated to hold 200000 tonnes of fluorite ore. The ore is exploited by the simple method of selective mining and hand-picking by local laborers. The hand-picked ore is then stockpiled before being sent to the Isfahan steel mill where it is used as a fluxing agent.

A recent study by Sadeghi [10] indicates that the mineralization occurs as a single-stage hydrothermal event. The main focus of this paper is to determine the physico-chemical characteristics of fluids responsible for the fluorite and lead mineralization as attested by fluid inclusion studies and to establish the overall condition of mineralization at the Kamar-Mehdi mine.

Sample Preparation

Considering the fact that fluorite is the only transparent ore mineral in the Kamar-Mehdi mine, all fluid inclusion microthermometric measurements were carried out on this mineral. It is also assumed that deposition of the coexisting (cogenetic ?) galena has taken place within the temperature range of fluorite deposition. Systematic sampling at the Kamar-Mehdi mine was carried out along and perpendicular to the exposed fluorite veins at the present level of erosion and also different levels of underground tunnels. Doubly-polished wafers were prepared from the collected samples using mount resin and thin-section methods [3,9,12].

The microthermometric studies were made with a Linkam HFS91 combined heating and freezing stage. Calibration during freezing was against distilled water (0°C), carbon tetrachloride (-22.8°C) and chloroform (-63.5°C), and during heating against potassium nitrate (335°C), potassium dichromate (398°C) and benzoic acid (122°C). The accuracy of measured values is +0.5°C for freezing and +0.1°C for heating.

A rapid method of leaching the inclusion fluids was followed: Approximately 100 grams of fluorite was

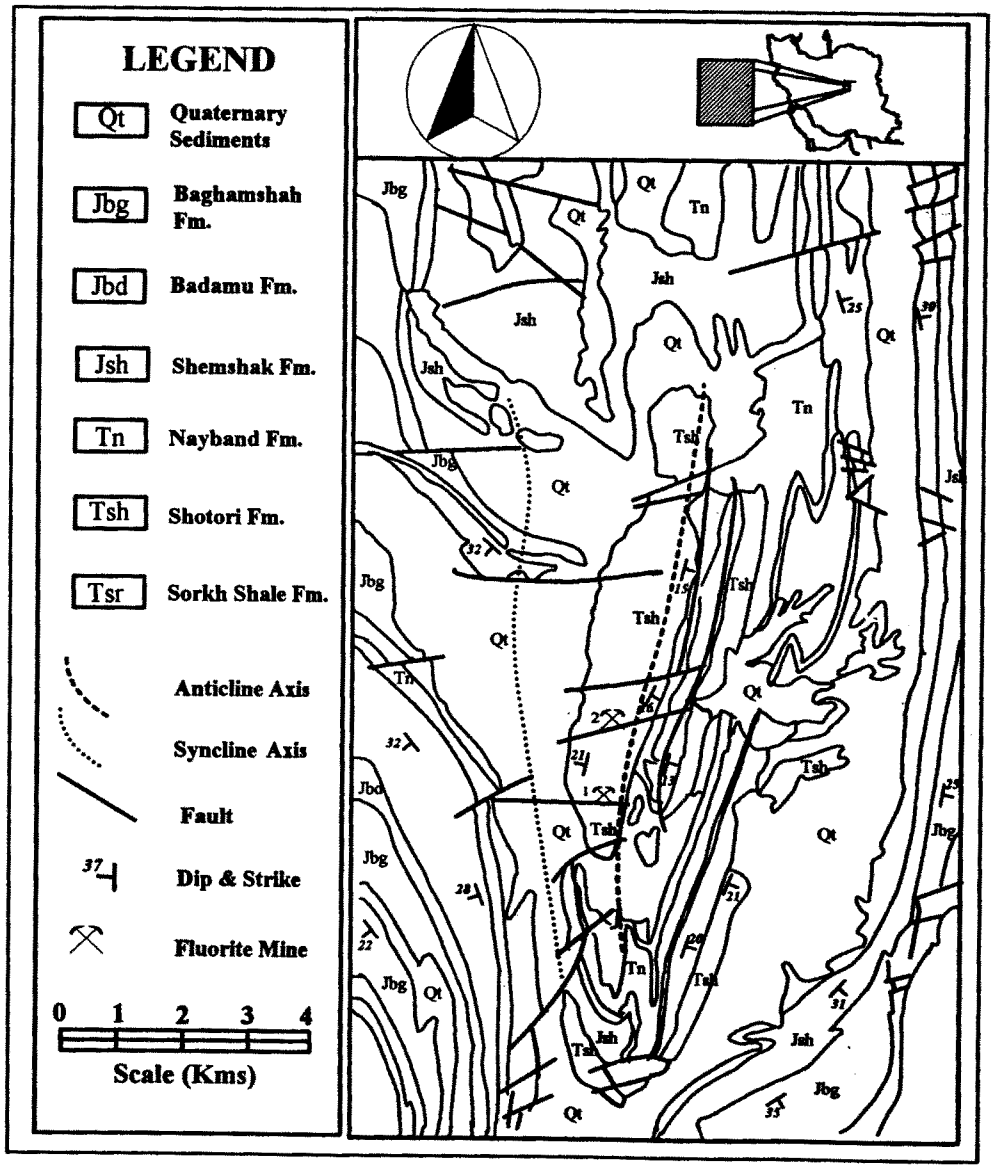

Figure 2. Photogeological map of Kamar-Mehdi anticline (modified after Sadegi 1995)

selected from each level and after several stages of acid wash and sequential grinding, 20 grams of each specimen with an average grain size of 0.25 mm was hand-ground under a minimum amount of deionized distilled water, using an agate mortar and pestle. The resultant slurry was filtered, centrifuged and diluted to 25 ml. The leachates were then analyzed for cations of interest using standard flame emission and atomic absorption spectroscopic method.

Results and Discussion

Using the classifications of Nash and Theodor [7] and Roedder [9], Kamar-Mehdi fluid inclusions can morphologically be divided into four distinct types:

1- Monophase liquid inclusions
2- Monophase gaseous inclusions
3- Two phase liquid-vapor inclusions
4- Three phase liquid-vapor-daughter mineral inclusions

The third and fourth type represent the most and least abundant types, respectively. The degree of filling of inclusions also varies from 100% for the first type to almost zero for the second. However, the degree of filling of the majority of inclusions ranges between 92-97%. The

Table 1. Chemical composition of leachates (mg/l)

Elevation	Mine No.	Na	K	Ca	Mg	Na/K	Na/Ca	Na/Mg
1475	1	1.57	1.26	12.31	0.52	1.24	0.12	3.01
1424	1	1.02	0.63	31.02	0.28	1.61	0.03	3.64
1280	2	0.19	0.35	6.08	0.38	0.54	0.03	0.50
1485	1	0.60	0.53	7.10	0.35	1.13	0.08	1.71
1427	1	1.65	0.80	7.14	0.60	2.06	0.23	2.75
1420	1	3.15	0.63	5.88	0.28	5.00	0.53	11.25
1270	2	2.80	0.94	17.45	0.77	2.97	0.16	3.63
1220	3	1.17	0.88	7.11	0.44	1.32	0.16	2.48

inclusions appear in various sizes and shapes including lath-shape, bar shape, negative crystal-shape and irregular. The largest observed fluid inclusion measures 100 microns in size and the smallest one just over 3 microns. Some inclusions display evidence of necking down. Figure 4 represents some of the inclusions encountered in fluorite crystals at Kamar-Mehdi mine No. 1.

Frequency histograms for homogenization and last ice melting temperatures of about 1300 primary and pseudosecondary inclusions from mines No. 1 and 2 are depicted in Figure 5. Homogenization was mostly to a liquid phase but a few inclusions homogenized to a gaseous phase. Also, a number of inclusions decrepitated before reaching homogenization temperature. Upon freezing, the bubble of some inclusions disappeared and then reappeared again on the last ice melting point, indicating their metastability [9]. The reported homogenization temperatures are uncorrected for pressure, as the morphology of the inclusions and the open space nature of mineralization indicate that mineralization took place at rather shallow depths where pressure correction can not change the measured homogenization temperatures significantly and hence was considered negligible.

Figure 5 and Table 1 show that in mine No. 1 mineralization has taken place in a temperature range of 80 to 150°C with a conspicuous peak at 125°C. In mine No. 2, homogenization temperature ranges from 70 to 150°C with a prominent peak at 115°C.

The last ice melting temperatures of the liquid phase in mine No. 1 range from between -2.2°C to -0.4°C with -1.1°C being the most frequent. This melting range corresponds to a salinity of 0.7 to 3.69 equivalent weight percent NaCl. In mine No. 2, last ice melting temperatures range from between zero to -1.7°C with -0.9°C being the most frequent. This temperature corresponds to a salinity of 2.88 equivalent w.t.%NaCl.

Figure 6 indicates that homogenization temperature decreases with increasing elevation while salinity remains more or less unchanged, probably indicating the upward movement of mineralizing fluids.

The results of leachate analyses are presented in Table 2. Each reported value is the average of at least four individual specimens. No significant difference in leachate concentration was found to exist between different levels of the same mine or between mines No. 1 and 2. Also, no meaningful relationship exists between different ions. However, all analyzed specimens show a low Na/Ca ratio, indicating a high Ca content of the mineralizing fluid. This is not unusual considering the high carbonate content of the host, and the interaction between the mineralizing fluid and the wall rock. The rather high Ca/Mg ratio is also noticeable, probably indicating that Ca is more easily leached from the host by the mineralizing fluid. Analyses using á scanning electron microscope coupled with an energy dispersive unit have shown that the majority of daughter minerals fall within one of the two following types: an Si-K-Ca phase, and an Si-Cl, Al, K, Ca bearing phase. Some trapped crystallites of fluorite were also detected. Attempts to identify the daughter minerals, using a combination of morphological and chemical information, were futile, However, it is suspected that some daughter phases are probably calcium-bearing silicates (Wollastonite ?).

In order to study the REE composition of the fluorite ore of the Kamar-Mehdi mine, four specimens from mine No. 1 (KMF1-KMF4), and two specimens from mine No.

		Early — Late
Pre Ore Stage	Dolomite	
	Pyrite	
	Quartz	
Ore Stage	Galena	
	Fluorite	
	Magnetite	
	Hematite	
Post Ore Stage	Cerussite	
	Anglesite	
	Covellite	
	Azurite	
	Malachite	

Figure 3. Paragenetic sequence of mineralization at Kamar-Mehdi mine

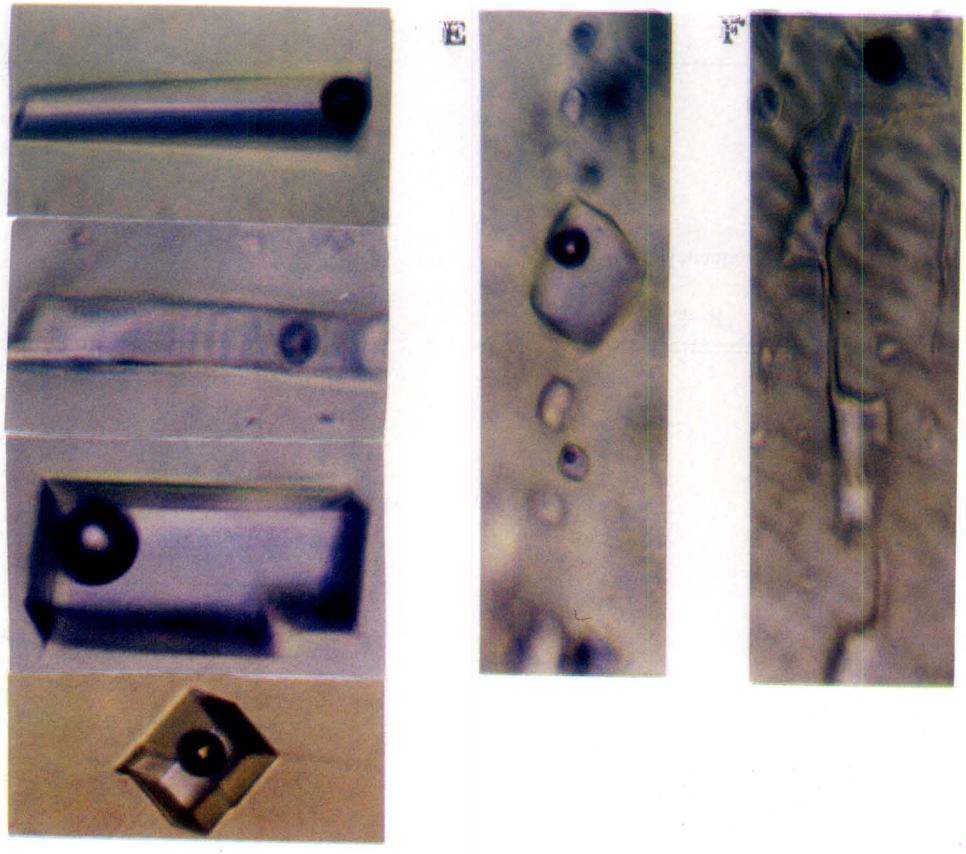

Figure 4. Different types of Kamar-Mehdi fluid inclusions: A,B,C and D are needle-shaped, lath-shaped and inclusions with negative crystal shapes respectively, E is a trail of secondary inclusions and F is a necked-down inclusion (magnification for all inclusions is 500)

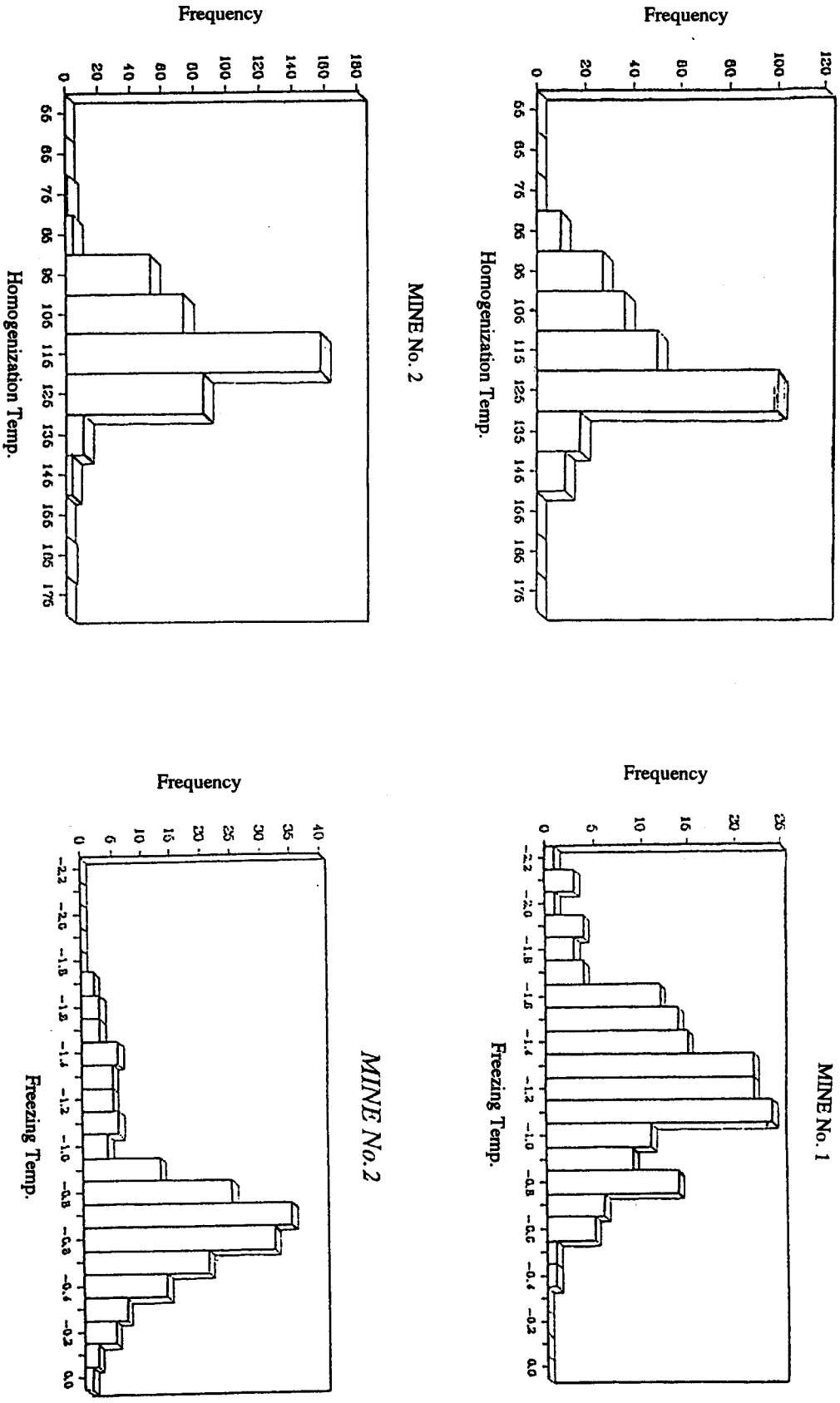

Figure 5. Homogenization and last ice melting temperatures of fluid inclusions in fluorite ore at the Kamar-Mehdi anticline

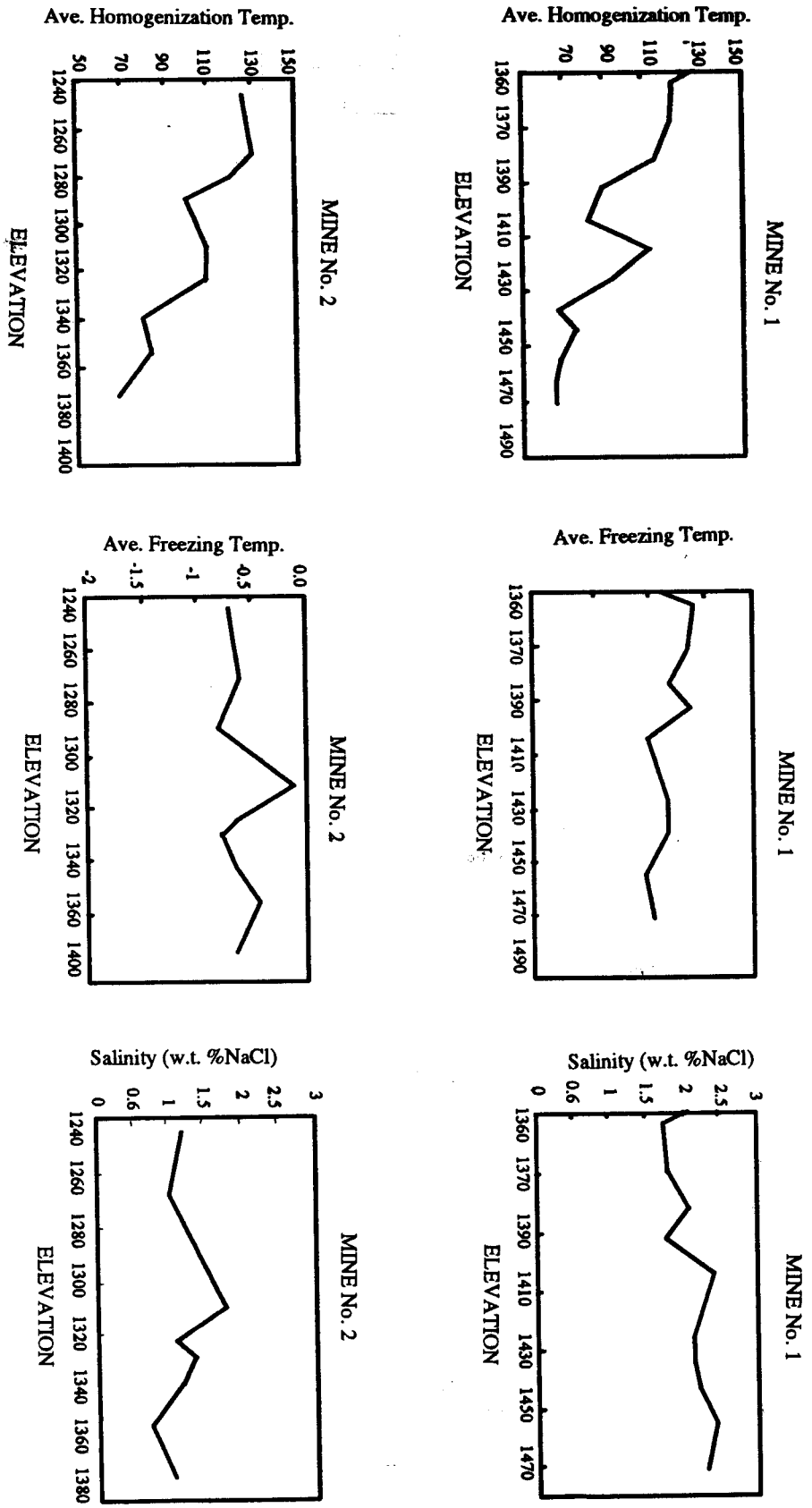

Figure 6. Variation of homogenization temperatures, last ice melting and salinity of fluid inclusions with elevation

Table 2. Rare earth element (REE) composition of Kamar-Mehdi fluorite (ppm)

Sample No.	KMF1	KMF2	KMF3	KMF4	KMF5	KMF6
La	1.66	1.33	2.15	1.14	21.25	1.45
Ce	3.93	1.49	n.d	0.44	n.d	3.36
Pr	0.30	0.34	0.38	0.09	0.12	0.28
Nd	2.16	3.29	68.74	1.65	31.24	6.39
Sm	1.20	0.37	0.30	0.12	0.90	0.83
Eu	0.16	0.09	0.12	0.04	0.022	0.14
Gd	4.79	1.94	n.d	1.30	n.d	2.11
Tb	0.09	0.15	0.06	0.013	0.19	0.11
Dy	0.68	0.18	0.40	0.054	0.077	0.07
Ho	0.11	0.05	n.d	0.024	0.48	0.03
Er	*	*	*	*	*	*
Tm	n.d	0.29	n.d	n.d	n.d	0.21
Yb	0.19	0.12	0.64	0.11	n.d	0.15
Lu	0.027	0.014	n.d	0.018	n.d	0.02
Ce/Yb	20.68	12.41		4.00		22.40
ΣREE	15.31	9.65	72.79	4.99	54.57	15.15

*Peaks of samples have been seen, but there was not a standard sample for comparison.
n.d: Not detected

2 (KMF5-KMF6) were collected from hand-picked stockpiles nearby. Care was taken to choose the purest samples free of any visible gangue or other impurities. After grinding, an aliquot of each specimen was sent to the Bureau of Atomic Energy of Iran for determination of REE by neutron activation analysis. The results are presented in Table 2.

Recent studies [6,8,11] have shown that REE/Ca and Tb/La ratio can confidently be used to reveal the origin of fluorite deposits [11]. Figure 7 presents a Tb/Ca versus Tb/La diagram. It can be seen that the Kamar-Mehdi specimens plot in the hydrothermal field of the diagram. The rather high Ce/Yb ratio indicates enrichment in light REE and hence the late origin of the mineralizing fluid. The variable content of REE in the analyzed samples is a common feature in all hydrothermal fluorites [2].

The chondrite normalized pattern of REE is presented in Figure 8. Data obtained by Wakita *et al.* [18] are used for normalization. The pattern is similar for all specimens with a strong positive anomaly for Eu and Dy and a strong negative anomaly for Nd, Tm and Gd. The positive Eu anomaly is probably caused by Eu^{+2} substitution for Ca^{+2} or Sr^{+2} ions in the fluorite lattice. In this case, a prevailing reducing condition must be suspected during mineralization of fluorite. The similarity of the patterns from mines No. 1 and 2 indicate a common origin.

Conclusion

From the foregoing it may be suggested that fluorite mineralization and the closely associated lead

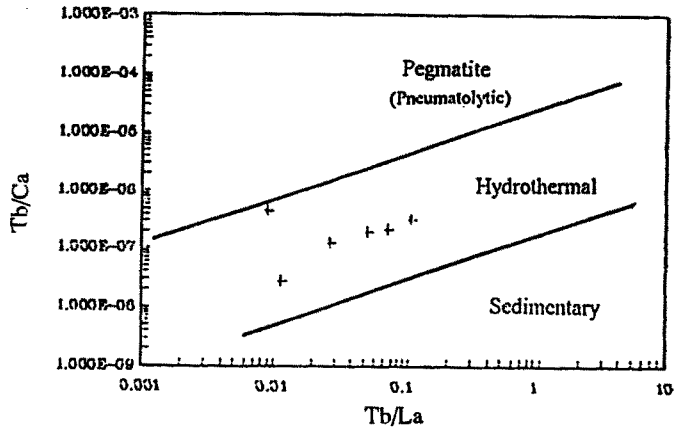

Figure 7. Tb/Ca versus Tb/La diagram. Note that all analyzed fluorite samples from Kamar-Mehdi mine plot are in the hydrothermal region of the diagram.

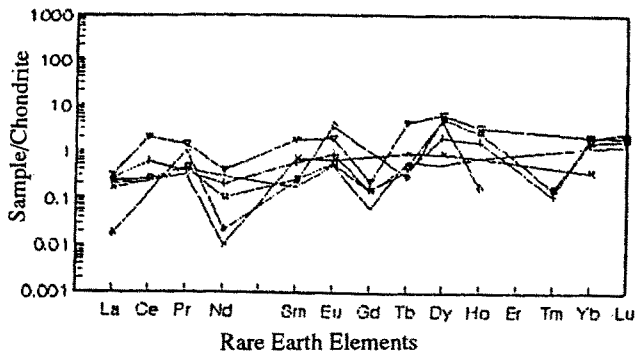

Figure 8. Chondrite normalized pattern of REE composition of Kamar-Mehdi fluorite

mineralization have taken place in a single episode between 70 to 150°C. Geochemistry of REE indicates a common hydrothermal source for mines No. 1 and 2. It seems likely that mineralization is structurally controlled and that the veins occupy E-W trending fault planes.

Acknowledgements

The authors would like to thank the Research Council of Shiraz University for financially supporting this project. Thanks are also extended to the Bureau of Atomic Energy of Iran for their help in REE analysis.

References

1. Berberian, M. Tectonic and sismotectonic sections; Contribution of sismotectonics of Iran, Part II, Rep. No. 39, p. 516, (1976).
2. Constantopoulos, J. Fluid inclusions and rare earth element geochemistry of fluorite from south-central Idaho. *Econ. Geol.*, **83**, 626-636, (1988).
3. Craig, J.R. and Vaughan, D.J. *Ore microscopy and ore petrography*, p. 406. John Wiley, New York, (1981).
4. Darvishzadeh, A. *Geology of Iran*, p. 901, (In Farsi). Neda Publication, (1992).
5. Holland, R.A.G., Bluy, C.J. and Spooner, E.T.C. A method for preparing doubly-polished thin section suitable for microthermometric examination of fluid inclusion. *Min. Mag.*, **42**, 407-408, (1978).
6. Moller, F., Parkh, P.P. and Schneider, H.J. The application of Tb/Ca-Tb/La abundance ratio to problems of fluorspar genesis. *Min. Dep.*, **11**, 111-116, (197--).
7. Nash, J.T. and Theodor, T. Ore fluids in the porphyry copper deposit at copper canyon. *Econ. Geol.*, **66**, 385-399, (1971).
8. Ohle, E.L. Some considerations in determining the origin of ore deposits of the Mississippi valley type, part II. *Econ. Geol.*, 161-172, (1980).
9. Reodder, E. *Fluid inclusion; Reviews in mineralogy*, Vol. 12. Min. Soci. of Am., Book Crafters, Inc., Michigan, (1984).
10. Sadeghi Bojd, M. Origin of lead mineralization in Shotori Formation, Tabas area-Khorasan Province. Unpublished M.Sc. thesis, Shiraz University, Iran, (1995).
11. Schneider, H.J., Moller, P. and Parekh, P.P. Rare earth elements distribution in fluorites and carbonate sediments of the East-Aloine mid-Triassic sequences in Nordlich Kalkalpen. *Min. Dep.*, **10**, 330-344, (1975).
12. Shepherd, T.J., Rankin, A.H. and Alderton, D.H.M. *A practical guide to fluid inclusion studies*, p. 239. Blackie, Glasgow and London, (1985).
13. Stockline, J., Eftekhar-Nezhad, J. and Hushmand Zadeh, A. *Geology of the Shotori range*. Geol. Sur. of Iran, Rep. No. 3, (1965).
14. Stockline, J. and Sotodehnia, A. *Stratigraphic lexicon of Iran*, (2nd edn). Geol. Sur. of Iran, Rep. No. 18, (1977).
15. Stockline, J., Eftekhar-Nezhad, J. and Hushmand Zadeh, A. *Preliminary investigation of central Lut geology, East Iran*. Geol. Sur. of Iran, Rep. No. 22f, (1972).
16. Takin, M. Iranian geology and continental drift in the Middle East. *Nata*, **235**, 147-150, (1972).
17. Tehrani, K. *General aspects of the stratigraphy of Iran and type sections of formations*. Tehran University Press. (In Farsi), (1988).
18. Wakita, H., Rey, P. and Schmitt, R.A. Abundances of the 14 rare earth elements and four soils. *Proc. 2nd Lunar Sci. Conf.*, 1319-1329, (1971).